Rose-Hulman Undergraduate Mathematics Journal

Volume 24
Issue 2

Article 12

Eigenvalue Algorithm for Hausdorff Dimension on Complex Kleinian Groups

Jacob Linden
University of Washington, jacob.linden@gmail.com

Xuqing Wu
University of Washington, xuqingwu@upenn.edu

Eigenvalue Algorithm for Hausdorff Dimension on Complex Kleinian Groups

Cover Page Footnote

We would like to thank Dr. Hadrian Quan and PhD student Raghavendra Tripathi for their teaching, guidance, and mentorship through this project. We also wish to thank the Washington Experimental Mathematics Lab and Professor Christopher Hoffman for supporting our research.

ℝose-Hulman Undergraduate Mathematics Journal
VOLUME 24, ISSUE 2, 2023

Eigenvalue Algorithm for Hausdorff Dimension on Complex Kleinian Groups

By *Jacob Linden* and *Xuqing Wu*

Abstract. In this manuscript, we present computational results approximating the Hausdorff dimension for the limit sets of complex Kleinian groups. We apply McMullen's eigenvalue algorithm [5] in symmetric and non-symmetric examples of complex Kleinian groups, arising in both real and complex hyperbolic space. Numerical results are compared with asymptotic estimates in each case. Python code used to obtain all results and figures can be found at `https://github.com/WXML-HausDim/WXML-project`, all of which took only minutes to run on a personal computer.

1 Introduction and Background

To motivate the concept of Hausdorff dimension, we begin by recalling the ternary Cantor set. Start with the unit interval $\mathrm{I}_0 = [0,1]$. Next, consider $\mathrm{I}_1 = [0,1/3] \cup [2/3,1]$ obtained by removing the middle third of this interval, leaving two intervals remaining. In the next step, we remove the middle third from each of the previous two intervals; proceeding iteratively in this manner, we obtain a family of sets $\{\mathrm{I}_n\}_{n\in\mathbb{N}}$. The common intersection of these sets,

$$\mathscr{C} = \bigcap_{n=0}^{\infty} \mathrm{I}_n,$$

is the ternary Cantor set. This resulting collection of points has Euclidean length zero, and is of topological dimension zero. In contrast, it can be shown that the Hausdorff dimension of this set is $\log_3(2) \approx 0.631$ (see [4]).

In general, most notions of the dimension of a set encode information about how the size of that set changes as it is scaled. When the interval $[-1,1]$ is scaled by a factor of 2, its length doubles. When the unit disk $\mathbb{D}$ is scaled by a factor of 2 along each axis, its area quadruples. Generally, when the unit n-ball,

$$\mathrm{B}^n = \{\mathbf{x} \in \mathbb{R}^n : |\mathbf{x}| \leq 1\},$$

is scaled by 2, its volume scales by 2^n. This exponent, n, is also the dimension of the n-ball.

Mathematics Subject Classification. 53A35
Keywords. Hyperbolic geometry, Heisenberg group, Kleinian group, Hausdorff dimension, dynamical systems, algorithms.

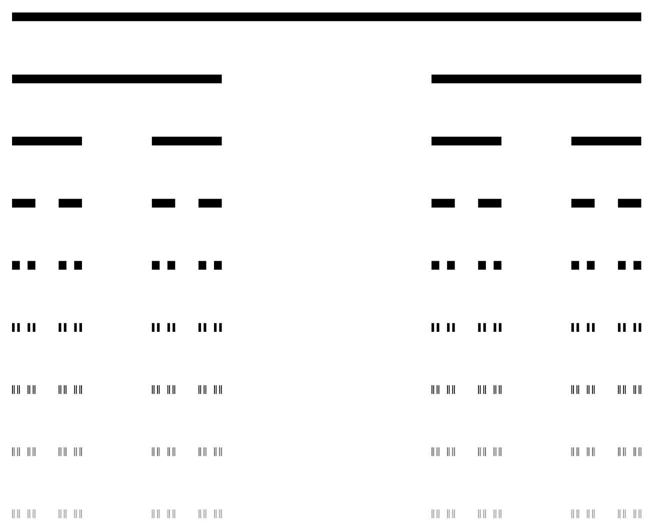

Figure 1: Construction of the Cantor set by iterations $I_0, I_1, \ldots$

However, for fractal sets such as Cantor sets, dimension is far more difficult to calculate, or to even define. In this paper, we use a notion of dimension called Hausdorff dimension. This dimension agrees with the dimension that one would expect for non-fractal sets, but can also be applied to fractal sets. On these fractal sets, we sometimes have non-integral Hausdorff dimension.

Going back to the example of the Cantor set, it can be shown that scaling the Cantor set by 2 scales its "volume" (more precisely, its Hausdorff measure) by a factor of $2^{\log_3(2)}$. Thus, Hausdorff dimension encodes information about volume-scaling, even for fractal sets. In this example of the Cantor set, we are able to obtain a closed-form expression for its Hausdorff dimension. However, for general fractal sets, this is difficult or impossible.

The fractals that we examine here are the limit sets of discrete subgroups of hyperbolic isometries (associated to both real and complex hyperbolic space, see §3 and §4 respectively). These groups, called *Kleinian groups*, are the subject of intense study [1, 2, 5, 6, 7, 8][1]. We start with such a Kleinian group, and iterate its action on a set in hyperbolic space, resulting in a set with finer and finer structure. The limit set on the boundary is obtained as we take the limit of this iteration process, yielding a set with infinitely fine structure, i.e., a fractal.

In figure 2, we provide a visualization of this iteration process, for the "symmetric pair of pants" Kleinian group from [5]. The darker region on the boundary, where circles

[1]We mention that the Kleinian groups considered in [5] and [6] are both referred to as *Schottky groups*, although strictly speaking neither of the examples considered therein meet the definition of a Schottky group.

of very small radius are accumulating, is exactly the limit set whose dimension we are computing.

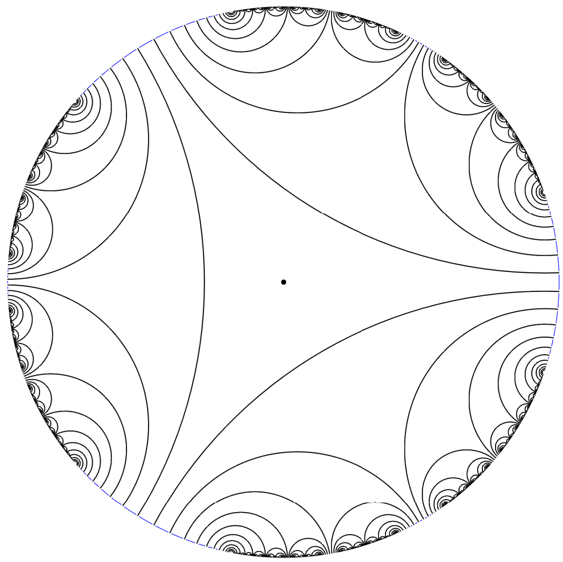

Figure 2: The dynamics of the symmetric pair of pants, for the arc angle $2\pi/3.1$. The limit set of this group has Hausdorff dimension approximately equal to 0.82694.

In [5], McMullen provides an effective method for computing the Hausdorff dimension of limit sets arising from Markov partitions (more on this in §2). This algorithm exhibits exponential convergence.

One type of Markov partition considered in this paper are those obtained by the action of *classical Kleinian groups*, which are groups of certain Möbius transformations (see §3 for details). Of particular interest are groups where each Möbius transformation corresponds to a reflection through a circle in the plane. One can think of this as an involution that fixes the circle, while continuously mapping its interior to its exterior, and its exterior to its interior.

The symmetric pair of pants example is a classical Kleinian group. Specifically, it is the group generated by reflections through a rotationally symmetric arrangement of three circles. For this example, McMullen gives an explicit asymptotic approximation to the Hausdorff dimension of its limiting set. Given a group of arc angle θ, the Hausdorff dimension of its limit set is approximated by

$$\alpha = \frac{\log 2}{\log 12 - 2\log\theta}.$$

We compare this asymptotic estimate to numerical results obtained via the eigenvalue algorithm in figure 4.

We also consider a non-symmetric Kleinian group, and derive our own approximation to the Hausdorff dimension. For a group of arc angle θ, an approximation α to the Hausdorff dimension of the group's limit set is given implicitly by

$$\frac{\theta^{2\alpha}}{2}\left(2^{-4\alpha}+\sqrt{2^{3-6\alpha}+2^{-8\alpha}}\right)=1.$$

See figure 6 for a comparison with numerical results.

At this point, a fair amount of study has been devoted to classical Kleinian groups associated to two-dimensional real hyperbolic space, and to the Hausdorff dimension of their limit sets. We also consider the generalization of this to two complex dimensions (see §4). In this setting, we consider the functions that act as analogues of a Möbius transformation, and call the group generated by them a *higher dimensional complex Kleinian group*. Comparatively less is known about such complex Kleinian groups, but there are a few papers, including [6], that explore the topic.

Given a symmetric complex Kleinian group with 3 generators, Romaña and Ucan-Puc [6] give an asymptotic estimate to the dimension of its limit set. For a group of arc angle θ, the Hausdorff dimension is approximated by

$$\alpha=\frac{\log 2}{\log 12-4\log\sin(\theta)}.$$

See figure 9.

We also consider a non-symmetric case. We derive our own approximation to the Hausdorff dimension: for a group of arc angle θ, an approximation α to the Hausdorff dimension of the group's limit set is given implicitly by

$$\frac{\sin^4(\theta)}{2}\left(2^{-2\alpha}+\sqrt{2^{3-2\alpha}+2^{-4\alpha}}\right)=1.$$

See figure 11.

1.1 Hausdorff Measure and Dimension

In order to define the Hausdorff dimension of a set, we must first define an associated measure. Typically, one uses the Lebesgue measure to measure subsets of $\mathbb{R}^n$. This measure is equal to the n-dimensional volume that we expect for such sets. For our purposes, we use a generalization of the Lebesgue measure, called the Hausdorff measure. This measure is defined as a limit of pre-measures, in the following way.

Definition 1.1. Given a subset S of a metric space, and real numbers $\alpha,\delta>0$, a Hausdorff pre-measure for S is given by

$$\mathrm{H}^{\delta}_{\alpha}(\mathrm{S})=\inf_{\mathscr{U}}\left\{\sum_{j=1}^{\infty}(\operatorname{diam}\mathrm{U}_j)^{\alpha}\right\},$$

where the infimum is taken over all countable open covers $\mathscr{U}$ of S, and the open sets U_j of $\mathscr{U}$ satisfy $\operatorname{diam} U_j < \delta$.

Definition 1.2. The α-dimensional Hausdorff measure of S is

$$H_\alpha(S) = \lim_{\delta \to 0} H_\alpha^\delta(S).$$

One can think of taking δ to 0 as capturing the roughness of the set S in increasing detail. As the diameter of each open set U_j is further restricted, the cover $\mathscr{U}$ becomes less course.

Definition 1.3. Given a subset S of a metric space, the Hausdorff dimension of S is the unique value α_0 such that $H_\alpha(S) = \infty$ for $\alpha < \alpha_0$, and $H_\alpha(S) = 0$ for $\alpha > \alpha_0$.

1.2 Dynamical Systems and Limit sets

Now that we have defined Hausdorff dimension, we say a bit more about the setting in which the fractal sets of interest arise. What follows are a few definitions that will be of use.

Definition 1.4. A *dynamical system* Γ on a set S is a collection of maps

$$\gamma_a : U_a \to S,$$

where $U_a \subset S$ is open.

The collection Γ need not be finite, or even countable. A dynamical system is said to be *conformal* if each of its constituent maps γ_a is conformal, that is, angle-preserving.

A function γ is said to be a *contraction* on a metric space (X, d) if there exists some constant $\xi < 1$ such that for any $x_1, x_2 \in X$,

$$d(\gamma(x_1), \gamma(x_2)) \leq \xi \cdot d(x_1, x_2).$$

Given a subset U of a topological space V, $x \in V$ is called a *limit point* of the set U if every neighborhood of x contains a point in U that is different from x.

Given a dynamical system Γ, the *orbit* of a point $x \in S$ is defined as

$$\Gamma_x = \{\gamma_a(x) : \gamma_a \in \Gamma\}.$$

Definition 1.5. Given a dynamical system Γ on a set S, its *limit set* $\Lambda(\Gamma)$ is the set of limit points of all orbits Γ_x, $x \in S$.

In this paper, we seek to estimate the Hausdorff dimension of the limit sets of dynamical systems: specifically, the action of complex Kleinian groups on hyperbolic space. As will be seen in the next section, if the generators of the Kleinian group act as contractions on certain pieces of their domain, we can use McMullen's eigenvalue algorithm to obtain an accurate estimate of the Hausdorff dimension.

2 The Eigenvalue Algorithm

2.1 Overview

McMullen's eigenvalue algorithm was introduced in [5] to provide a method for computing the Hausdorff dimension of fractal sets arising from a variety of problems of geometric interest. Beginning with a conformal dynamical system, one iteratively produces a sequence of matrices T. At each iteration, there exists an exponent α such that the largest eigenvalue of T^α is 1. The value α at each stage provides a good approximation to the true dimension. Specifically, N digits of accuracy are obtained in $\mathcal{O}(N)$ iterations.

2.2 Markov Partitions

A *Markov partition* is a nonempty collection $\{(P_i, f_i)\}$ of compact connected sets P_i and maps f_i defined on each P_i, satisfying a few properties. Denote the domain of Γ by $D = \cup P_i$. Given a conformal dynamical system Γ, a Γ-invariant density of dimension δ is a finite, positive measure μ such that

$$\mu(f(S)) = \int_S |f'(x)|^\delta \, d\mu, \tag{1}$$

whenever $S \subset D$ is a Borel set such that $f \in \Gamma$ is injective on S. Then, a Markov partition is required to satisfy the following:

1. $f_i(P_i) \supset \bigcup_{i \mapsto j} P_j$, where $i \mapsto j$ means that $\mu(f_i(P_i) \cap P_j) > 0$.
2. When $i \mapsto j$, there exists a neighborhood U of $P_i \cap f_i^{-1}(P_j)$ such that f_i is homeomorphic on U.
3. For all i, $\mu(P_i) > 0$.
4. For all $i \neq j$, $\mu(P_i \cap P_j) = 0$.
5. For each i, $\mu(f_i(P_i)) = \mu(\bigcup_{i \mapsto j} P_j)$.

In the above conditions, note that the images of the P_i under the f_i are restricted to the domain D of Γ. The last of these conditions is a measure-preserving property.

A Markov partition is called *expanding* if there exists $\xi > 1$ such that $|f_i'(x)| \geq \xi$ for $x \in P_i \cap f_i^{-1}(P_j)$. In particular, note that f_i^{-1} is a contraction on P_j if and only if f_i is expanding on $P_i \cap f_i^{-1}(P_j)$. This leads us to the following convergence theorem:

Theorem 2.1 ([5])**.** Given an expanding Markov partition for a conformal dynamical system, suppose that the limiting set of this system has Hausdorff dimension δ. Then, the eigenvalue algorithm requires at most $\mathcal{O}(N)$ refinements to approximate δ to N digits of accuracy.

A classical Kleinian group is expanding when considered as a Markov partition. However, complex Kleinian groups are not necessarily expanding. The following theorem allows us to apply McMullen's results to the complex case.

Theorem 2.2 ([6])**.** Given a Markov partition (P_i, f_i) corresponding to a complex Kleinian group acting on $\mathbb{H}^2_{\mathbb{C}}$, suppose that there exists $\xi > 1$ and $M \in \mathbb{N}$ such that the matrix defined by

$$J^M_{f_i}(x_1, x_2, x_3) = \left\{ \frac{\partial^M f_{i,j}}{\partial x_k^M} \right\}_{j,k=1,2,3}$$

satisfies

$$\min_{(x_1,x_2,x_3)\in\cup_j P_j} \left|\det\left(J^M_{f_i}(x_1, x_2, x_3)\right)\right| \geq \xi,$$

where $f_{i,j}$ denotes the j-th entry of the map f_i. Then, the results of theorem *2.1* hold.

2.3 McMullen's Algorithm

Given a complex Kleinian group with sets P_i, let f_i denote the reflection through P_i. This forms a Markov partition $\Gamma = (f_i, P_i)$, with some Γ-invariant density μ. Take sample points $x_i \in P_i$. Following [5], we write $i \mapsto j$ to mean that $\mu(f_j(P_i) \cap P_j) > 0$. In our particular case, this is equivalent to the requirement that $f_j(P_i) \subset P_j$. It should also be noted that reflections are involutions, so $f_i = f_i^{-1}$ for every i. The steps of the algorithm are as follows:

1. For each i, j such that $i \mapsto j$, compute y_{ij} such that $f_i(y_{ij}) = x_j$.

2. Compute and store the transition matrix T, where

$$T_{ij} = \begin{cases} \frac{1}{|f_i'(y_{ij})|} & i \mapsto j, \\ 0 & \text{otherwise.} \end{cases}$$

3. Find α such that the largest eigenvalue in absolute value (the spectral radius) of the element-wise exponentiated matrix T^α is $\lambda(T^\alpha) = 1$.

4. Perform a refinement, replacing each P_i with its image under f_j with $i \mapsto j$. Define the y_{ij} as the new sample points x_i. Repeat.

It should be noted that the maps f_i do not change when a refinement is performed. Each new set is assigned the reflection associated to the initial set in which it is contained.

We provide an argument as to why we might expect the exponent α in the above algorithm to provide a good approximation to the true Hausdorff dimension δ of a given limiting set. Define a vector $\mathbf{m}$ with entries $m_i = \mu(\mathrm{P}_i)$. Then, by the measure-preserving property,

$$m_i = \mu(\mathrm{P}_i) = \sum_{j:i\mapsto j} \mu\left(f_i^{-1}(\mathrm{P}_j)\right).$$

Then (1) implies that

$$m_i = \sum_{j:i\mapsto j} \int_{\mathrm{P}_j} \left|(f_i^{-1})'(x)\right|^{\delta} d\mu.$$

Finally, using the inverse function theorem to obtain a crude approximation to each integral, we obtain

$$m_i \approx \sum_j |f_i'(y_{ij})|^{-\delta} \mu(\mathrm{P}_j) = \sum_j \mathrm{T}_{ij}^{\delta} m_j.$$

Thus $\mathbf{m} \approx \mathrm{T}^{\delta}\mathbf{m}$, so $\lambda = 1$ is an approximate eigenvalue of T^{δ}. It can be shown that this is an upper bound for all other eigenvalues of T^{δ}. For an expanding Markov partition, not only is this approximation good enough, but it actually leads to exponentially fast convergence by theorem 2.1.

Instead of using Newton's method to solve the eigenvalue problem in step (3) as in [5], we use the bisection method. This comes at lower computational cost, but it is possible that Newton's method more effectively prevents the accumulation of small roundoff errors.

Below is pseudocode for our implementation of the eigenvalue algorithm. Assume that the function `ref(i,j)` has been defined as the reflection of the j-th sample point under the i-th map, and that the function `ref_prime(i,j)` defined similarly with reflection derivatives. Assume also that a function `bisec(T)` has been defined, which takes the transition matrix as input and outputs an approximation α_{P} to the Hausdorff dimension.

Algorithm 1 The Eigenvalue Algorithm

```
refinements ← 0
num_refinements ← number of refinements
N ← number of disks
x ← sample points

while refinements < num_refinements do
    y ← zeros(N, N)

    Step 1:
    for 0 ≤ i, j < N do
        if i ↦ j then
            y[i, j] ← ref(i, j)
        end if
    end for

    Step 2:
    T ← zeros(N, N)
    for 0 ≤ i, j < N do
        if i ↦ j then
            T[i, j] ← 1/|ref_prime(i, j)|
        end if
    end for

    Step 3:
    α_P = bisec(T)

    Step 4:
    x ← y
    N ← length(x)
    refinements ← refinements + 1
end while
```

3 Classical Kleinian Groups

3.1 The Real Hyperbolic Plane

There are several different ways of modeling real hyperbolic space. We first consider the Poincaré half plane model,

$$\mathbb{H}^2_{\mathbb{R}} = \{(x, y) \in \mathbb{R}^2 : y > 0\}.$$

Though this is a real space, it will sometimes be convenient to write points in this space as $z = x + iy$. Euclidean space is imbued with a familiar metric, lending itself to a notion of distance that is calculated using the Pythagorean theorem in Cartesian coordinates. In hyperbolic space, the metric is quite different. With this metric, the orientation-preserving isometries of $\mathbb{H}^2_{\mathbb{R}}$ are exactly the elements of

$$\mathrm{PSL}(2,\mathbb{R}) = \left\{ \begin{pmatrix} a & b \\ c & d \end{pmatrix} \in \mathbb{R}^{2\times 2} : ad - bc = 1 \right\} \Big/ \{\pm \mathrm{I}\},$$

considered as Möbius transformations. Specifically, to map elements of $\mathrm{PSL}(2,\mathbb{R})$ to $\mathrm{Isom}(\mathbb{H}^2_{\mathbb{R}})$, we use the natural mapping

$$\begin{pmatrix} a & b \\ c & d \end{pmatrix} \mapsto \frac{az+b}{cz+d}.$$

It can be shown that this map is an isomorphism.

We can also realize this map in homogeneous (or projective) coordinates. Define the equivalence class of $(z_1, z_2) \in \mathbb{C}^2$ as

$$[z_1 : z_2] = \left\{(w_1, w_2) \in \mathbb{C}^2 \setminus \{0\} \mid (w_1, w_2) = (\alpha z_1, \alpha z_2), \alpha \in \mathbb{C}\right\}$$

The complex projective line is defined as

$$\begin{aligned} \mathbb{P}^1_{\mathbb{C}} &= \left\{[z_1 : z_2] \mid (z_1, z_2) \in \mathbb{C}^2 \setminus \{0\}\right\} \\ &= \left\{[z : 1] \mid z \in \mathbb{C}\} \cup \{[1 : 0]\right\}. \end{aligned}$$

Then, a Möbius transformation acts on $\mathbb{P}^1_{\mathbb{C}}$ by

$$[z : 1] \mapsto [az + b : cz + d] = \left[\frac{az+b}{cz+d} : 1\right]$$

This is simply the equivalence class of

$$\begin{pmatrix} a & b \\ c & d \end{pmatrix} \begin{pmatrix} z \\ 1 \end{pmatrix}.$$

This is helpful in the sense that it allows a Möbius transformation to be applied directly via matrix multiplication.

The maps that we are interested in are reflections through circles that meet the boundary of hyperbolic space *orthogonally*. In the setting of the half plane, this is ensured by requiring that the center of the circle lies on the boundary, $\mathrm{Im}(z) = 0$.

It is a classical result that every Möbius transformation with $ad - bc \neq 0$ fixes some circle in the plane. If we require that a Möbius transformation fixes a given circle of radius r and center $a \in \mathbb{R}$, we obtain the reflection

$$\begin{pmatrix} a/r & -(r^2+a^2)/r \\ 1/r & -a/r \end{pmatrix} \cong \frac{az-(r^2+a^2)}{z-a}.$$

Simplification on the right side yields the maps

$$\rho(z) = a - \frac{r^2}{z-a}. \tag{2}$$

In some contexts, it is more convenient to instead use the Poincaré disk model of hyperbolic space. In this case, the real hyperbolic plane is identified with the open unit disk instead of the upper half-plane, that is, $\mathbb{H}_2^{\mathbb{R}} = \mathbb{D}$. In this case, the boundary is simply the unit circle. We can map from the disk model to the half plane with the Möbius transformation

$$\varphi(z) = -i \cdot \frac{z+1}{z-1},$$

and from the half plane model to the disk with its inverse

$$\varphi^{-1}(z) = \frac{z-i}{z+i}.$$

In the disk model, there is a somewhat different metric from the half plane, yielding a different set of isometries. Specifically, the isometries of the disk model are given by

$$\mathrm{PU}(1,1) = \left\{ \begin{pmatrix} u & \overline{v} \\ v & \overline{u} \end{pmatrix} \in \mathbb{C}^{2\times 2} : |u|^2 - |v|^2 = 1 \right\} \Big/ \{\pm \mathrm{I}\}. \tag{3}$$

When a point in the disk is represented as a complex number z, these isometries are applied as Möbius transformations, as in the half plane model.

We also again wish to obtain reflections through circles that meet the boundary orthogonally. In the case of the disk model, the requirement that a circle be centered on the boundary fails to produce this result. Given a point $c \in \mathbb{C} \setminus \overline{\mathrm{D}_1}$, the unique circle centered at c that intersects S_1 orthogonally is the circle of radius $\sqrt{|c|^2 - 1}$.

3.2 Classical Kleinian Groups

A discrete subgroup of $\mathrm{PSL}(2,\mathbb{C})$ is called a *classical Kleinian group*. In particular, a classical Kleinian group is called a *Fuchsian group* if it is a discrete subgroup of $\mathrm{PSL}(2,\mathbb{R})$.

Thus the elements of Fuchsian groups are isometries of hyperbolic space in the half-plane model. Since $\mathrm{PU}(1,1)$ is a subgroup of $\mathrm{PSL}(2,\mathbb{C})$, discrete subgroups of $\mathrm{PU}(1,1)$ are classical Kleinian groups.

In both models of $\mathbb{H}^2_{\mathbb{R}}$, we will further require that the generators of these groups are involutions, and that they fix a circle that lies orthogonal to the boundary $\partial\mathbb{H}^2_{\mathbb{R}}$. We will refer to these throughout as “reflections", due to their action of mirroring points across circles in hyperbolic space.

When operating in the disk model, we will often define a group in terms of the angle of the center of a circle, denoted θ, and the angle between the two points where the circle intersects S_1, denoted ϕ. Assuming that a circle intersects S_1 orthogonally, with a bit of computation we obtain the following formulas for the radius and center of a circle in terms of angles:

$$r = \tan\left(\frac{\phi}{2}\right), \quad c = \sec\left(\frac{\phi}{2}\right)e^{i\theta}. \tag{4}$$

Since $\phi > 0$ in order for r to be nonzero, we have that $|c| > 1$. Additionally, solving for r in terms of c gives us

$$r = \sqrt{|c|^2 - 1}.$$

The reflection through the circle of central angle θ and arc angle ϕ can be written explicitly in terms of this data, as in the half-plane. By requiring that the reflection fixes a given circle with $\theta \in [0,2\pi)$ and $\phi \in (0,\pi)$, we obtain the parameters u and v by

$$u = i\csc\left(\frac{\phi}{2}\right), \quad v = i\cot\left(\frac{\phi}{2}\right)e^{-i\theta}.$$

Combining this with (4), we can also write u and v in terms of the center and radius of the associated disk:

$$u = i\frac{|c|}{r}, \quad v = i\frac{\overline{c}}{|c|r}. \tag{5}$$

3.3 The Symmetric Pair of Pants

The symmetric pair of pants, as in [5], is defined in the disk model by first taking three disks of identical radii, such that the circle bounding each disk lies orthogonal to the boundary, the disks are pairwise disjoint, and the arrangement of disks is symmetric under rotation by $2\pi/3$. The symmetric pair of pants is then defined to be the classical Kleinian group generated by the reflections through these circles.

More explicitly, we construct a symmetric arrangement of circles by letting $\theta_1 = \pi/2$, $\theta_2 = 7\pi/6$, and $\theta_3 = 11\pi/6$ be the angles of the center of each circle in the group. We then define $\phi \in (0,2\pi/3)$ to be the angle of the arc contained in each disk. This arrangement is shown in figure 3.

Denote the reflection through the j-th circle by ρ_j. We would next like to derive an asymptotic estimate for the dimension of the limiting set of this group, as in Theorem 3.5

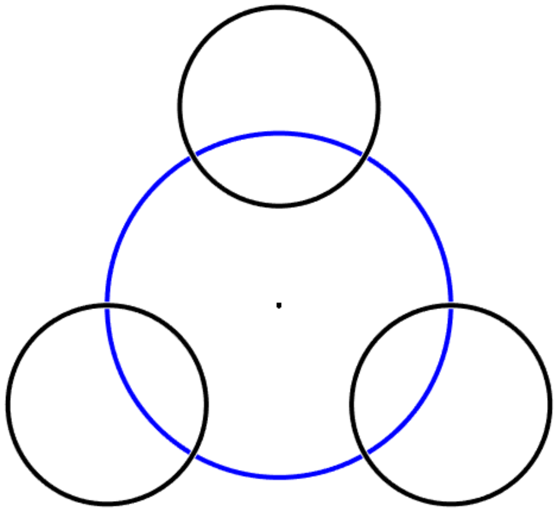

Figure 3: The symmetric pair of pants for $\phi = \pi/3$, with the unit circle shown in blue.

of [5]. For small angles ϕ, since the reflections ρ_j are nearly linear on $P_i \cap \rho_i(P_j)$, we obtain a close estimate to the true dimension in just one refinement. We estimate the entries of the transition matrix T, and solve for α in the equation $\lambda(T^\alpha) = 1$ (exponentiation applied element-wise).

Consider the reflection of the j-th disk in the group through the i-th disk, with $i \neq j$. We approximate the entries of T by evaluating ρ_i' at $z_j = e^{i\theta_j}$. This point z_j is the center of the arc of the unit circle contained in the j-th disk. Note in particular that for the symmetric group that we are considering, $\theta_j = \theta_i \pm \frac{2\pi}{3}$. We will also make the approximation $r_i \approx \frac{\phi}{2}$. By differentiating (3) and making the substitution in (4), we find that

$$\begin{aligned}|\rho_i'(z_j)| &= \left|\frac{1}{(vz_j + \overline{u})^2}\right| \\ &\approx \frac{r_i^2}{|\overline{c_i}z_j - 1|^2} \\ &\approx \frac{r_i^2}{|e^{\pm 2\pi i/3} - 1|^2} \\ &\approx \frac{\phi^2}{12}.\end{aligned}$$

Then, the entries of the transition matrix are given by

$$T_{ij}^\alpha = \begin{cases} \left(\frac{\phi^2}{12}\right)^\alpha & i \neq j, \\ 0 & i = j. \end{cases}$$

The spectral radius of T^α is $2\cdot\phi^{2\alpha}/12^\alpha$, and setting this equal to 1 yields the asymptotic formula

$$\alpha = \frac{\log 2}{\log 12 - 2\log\phi}.$$

Using the eigenvalue algorithm, we computed the Hausdorff dimension of the limiting set, for a variety of arc angles ϕ. We took three refinements in the algorithm. In figure 4, we compare the numerically computed dimension with the asymptotic estimate from above. The dimension is near zero for small angles, and is near 1 for angles close to

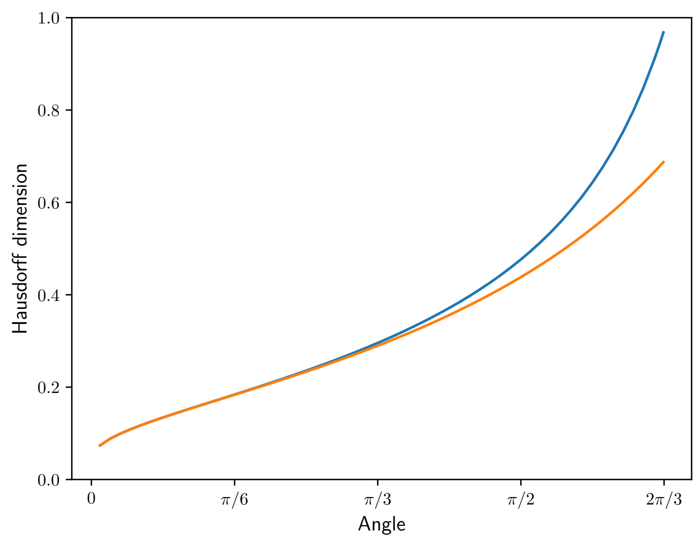

Figure 4: Numerically computed Hausdorff dimension (blue) and dimension estimated by the asymptotic formula (orange).

$\frac{2\pi}{3}$. This corroborates with expectation: a Kleinian group with generators of zero radius would have only the centers of the group as its limiting set, while the group of arc angle $\frac{2\pi}{3}$ has the entire unit circle as its limiting set. The asymptotic is highly accurate for small angles, but starts to diverge from the numerically computed dimension for larger angles, as we would expect.

3.4 Non-Symmetric Examples

The first non-symmetric example we consider is that with disks centered at angles $\theta_1 = \pi/2$, $\theta_2 = \pi$, and $\theta_3 = 3\pi/2$. For this group, it is necessary that the arc angle ϕ lies in $(0, \pi/2)$, since we require that the disks be disjoint. The group is shown in figure 5.

We now derive an asymptotic estimate using a method similar to that used in §3.3. The situation is slightly different from the symmetric case, in that the distances

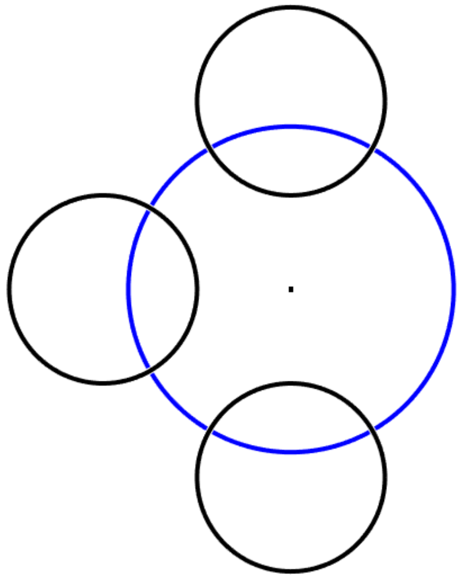

Figure 5: A non-symmetric Kleinian group, with $\phi = \pi/3$.

between the disks are not all identical. Thus, the structure of the transition matrix will not be as simple. We first consider pairs of adjacent disks, that is, those with $(i, j) \in \{(1,2),(2,1),(2,3),(3,2)\}$. In this case, if ρ_i denotes the reflection through the i-th disk, we have that

$$\begin{aligned} |\rho_i'(z_j)| &\approx \frac{r_i^2}{|\overline{c_i} z_j - 1|^2} \\ &\approx \frac{r_i^2}{|e^{\pm i\pi/2} - 1|^2} \\ &\approx \frac{\phi^2}{8}, \end{aligned}$$

where as before, we have used the approximation $r_i \approx \frac{\phi}{2}$. For the non-adjacent disks, where $(i, j) \in \{(1,3),(3,1)\}$, we have

$$\begin{aligned} |\rho_i'(z_j)| &\approx \frac{r_i^2}{|e^{\pm i\pi} - 1|^2} \\ &\approx \frac{\phi^2}{16}. \end{aligned}$$

Hence, we approximate the transition matrix as

$$T \approx \frac{\phi^2}{8}\begin{pmatrix} 0 & 1 & 1/2 \\ 1 & 0 & 1 \\ 1/2 & 1 & 0 \end{pmatrix}.$$

The largest eigenvalue of T^α is then

$$\frac{\phi^{2\alpha}}{2}\left(2^{-4\alpha} + \sqrt{2^{3-6\alpha} + 2^{-8\alpha}}\right) = 1. \tag{6}$$

This equation is quite difficult to solve analytically, but a numerical solution can be obtained quickly via root finding methods. Thus, we can use the solution to the above equation as an asymptotic estimate for dimension. We computed the Hausdorff dimension for a variety of angles ϕ for the Kleinian group, taking three refinements. These numerical values are compared with the asymptotic estimate, in figure 6.

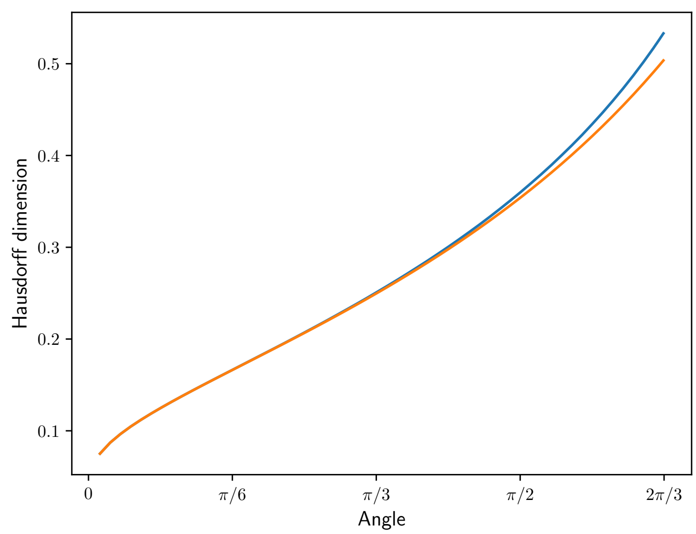

Figure 6: Numerically computed Hausdorff dimension (blue) and dimension estimated by asymptotic formula (orange).

4 Complex Kleinian Groups

4.1 The Complex Hyperbolic Plane and the Heisenberg Group

In complex hyperbolic space, we use the Siegel upper half-space model. This is analogous to the Poincaré half-plane model in the real case (see §3.1). First, define $\mathbb{C}^{2,1}$ as the vector space $\mathbb{C}^3$ with the Hermitian form

$$\left\langle \begin{pmatrix} z_1 \\ z_2 \\ z_3 \end{pmatrix}, \begin{pmatrix} w_1 \\ w_2 \\ w_3 \end{pmatrix} \right\rangle = \begin{pmatrix} \overline{z}_1 & \overline{z}_2 & \overline{z}_3 \end{pmatrix} \begin{pmatrix} 0 & 0 & 1 \\ 0 & 1 & 0 \\ 1 & 0 & 0 \end{pmatrix} \begin{pmatrix} w_1 \\ w_2 \\ w_3 \end{pmatrix} \tag{7}$$
$$= \left(\overline{z}_1 w_3 + \overline{z}_2 w_2 + \overline{z}_3 w_1 \right)$$

To obtain the Siegel upper half-space, we use homogeneous coordinates as in the Poincaré half-plane (see §3.2). To do this, set $z_3 \equiv 1$. We then define complex hyperbolic space with the following convention:

$$\mathbb{H}^2_{\mathbb{C}} = \left\{ \begin{pmatrix} z_1 \\ z_2 \\ 1 \end{pmatrix} \in \mathbb{C}^{2,1} : \mathrm{Re}(z_1) < -\frac{|z_2|^2}{2} \right\}$$

This convention, and many of the others we follow, is similar to that used in [6]. We will call the coordinates (z_1, z_2) *affine coordinates*.

The boundary of $\mathbb{H}^2_{\mathbb{C}}$, denoted $\partial\mathbb{H}^2_{\mathbb{C}}$, is of special interest. In particular, if we define

$$\begin{pmatrix} z_1 \\ z_2 \\ 1 \end{pmatrix} = \begin{pmatrix} -|\zeta|^2 + iv \\ \sqrt{2}\zeta \\ 1 \end{pmatrix},$$

then $\mathrm{Re}(z_1) = -\frac{|z_2|^2}{2}$ for all $\zeta \in \mathbb{C}$ and $v \in \mathbb{R}$. When considered in the coordinate system $(\zeta, v) \in \mathbb{C} \times \mathbb{R}$, the boundary $\partial\mathbb{H}^2_{\mathbb{C}}$ has the geometry of the Heisenberg group, $\mathscr{H}$. Throughout, we will consider $\partial\mathbb{H}^2_{\mathbb{R}} \cong \mathscr{H}$. Points in $\partial\mathbb{H}^2_{\mathbb{C}}$ are imbued with the group operation

$$(\zeta_1, v_1) * (\zeta_2, v_2) = \left(\zeta_1 + \zeta_2, v_1 + v_2 + 2\,\mathrm{Im}(\overline{\zeta_1}\zeta_2) \right). \tag{8}$$

Since the second coordinate is non-commutative, this is a non-abelian group.

There is also a notion of distance in the Heisenberg group: it is called the *Korányi gauge*, defined by

$$|(\zeta, v)|_0 = \left| |\zeta|^2 + iv \right|^{1/2}.$$

The Korányi gauge is also sometimes referred to as the Cygan norm, although strictly speaking it is not quite a norm, since it is not defined on a vector space.

Using this distance, we can define a metric on $\mathscr{H}$, called the *Cygan distance*:

$$\begin{aligned} d_{cyg}((\zeta_1, v_1), (\zeta_2, v_2)) &= |(\zeta_1, v_1) * (\zeta_2, v_2)^{-1}|_0 \\ &= \left| |\zeta_1 - \zeta_2|^2 + i(v_1 - v_2 - 2\,\mathrm{Im}(\overline{\zeta_1}\zeta_2)\right|^{1/2} \end{aligned}$$

This is a right-invariant metric on $\mathscr{H}$.

The non-affine coordinate system we have constructed thus far is extended to all of $\mathbb{H}^2_{\mathbb{C}}$ as follows: we write

$$\begin{pmatrix} z_1 \\ z_2 \\ 1 \end{pmatrix} = \begin{pmatrix} -|\zeta|^2 - u + iv \\ \sqrt{2}\zeta \\ 1 \end{pmatrix},$$

with

$$u := -\mathrm{Re}(z_1) - \frac{|z_2|^2}{2}.$$

We refer to the coordinates $(\zeta, u, v) \in \mathbb{C} \times \mathbb{R}^+ \times \mathbb{R}$ as *modified horospherical coordinates*. These are obtained from horospherical coordinates, as defined by Goldman and Parker in [3], via a linear fractional change of variable from affine coordinates. This choice helps to simplify notation.

Note that on $\mathbb{H}^2_{\mathbb{C}}$, we have $\mathrm{Re}(z_1) < -\frac{1}{2}|z_2|^2$, so $u > 0$. The set $u = 0$ coincides exactly with $\partial\mathbb{H}^2_{\mathbb{C}}$. We can now extend the definition of Cygan distance to the interior of complex hyperbolic space by defining

$$d_{cyg}((\zeta_1, u_1, v_1), (\zeta_2, u_2, v_2)) = \left| |\zeta_1 - \zeta_2|^2 + |u_1 - u_2| + i(v_1 - v_2 - 2\,\mathrm{Im}(\overline{\zeta_1}\zeta_2)\right|^{1/2}.$$

With this new notion of distance, we can define the objects which play a role analogous to the one circles played in the real case. The *Cygan sphere* of center (ξ, x, t) and radius r in the closure of $\mathbb{H}^2_{\mathbb{C}}$ is

$$\mathrm{S}_\lambda(\xi, x, t) = \left\{ \begin{pmatrix} -|\zeta|^2 - u + iv \\ \sqrt{2}\zeta \\ 1 \end{pmatrix} \in \overline{\mathbb{H}^2_{\mathbb{C}}} : d_{cyg}((\zeta, u, v), (\xi, x, t)) = r \right\}.$$

Note that these spheres are different from spheres defined with respect to the standard distance on $\mathbb{H}^2_{\mathbb{C}}$. Because we are primarily concerned with points in the boundary, since that is where the limit set will accumulate, we only consider spheres that are centered on the boundary of the space, i.e. by setting $x = 0$. Then, we take the intersection of such a sphere with the boundary. Writing the restriction of modified horospherical coordinates to $\partial\mathbb{H}^2_{\mathbb{C}}$ as $(\zeta, v) \in \mathbb{C} \times \mathbb{R}$, we define the Cygan sphere of center (ξ, t) and radius r in *the boundary* of $\mathbb{H}^2_{\mathbb{C}}$ as

$$\mathrm{S}_\lambda(\xi, t) = \left\{ \begin{pmatrix} -|\zeta|^2 + iv \\ \sqrt{2}\zeta \\ 1 \end{pmatrix} \in \partial\mathbb{H}^2_{\mathbb{C}} : d_{cyg}((\zeta, v), (\xi, t)) = r \right\}.$$

These are the objects through which we will be taking reflections.

Next, we discuss the isometries of $\mathbb{H}^2_{\mathbb{C}}$. The unitary group for the Hermitian form (7) is

$$\mathrm{U}(3,\mathbb{C}) = \{A \in \mathbb{C}^{3\times 3} : A^*BA = B\},$$

where

$$B = \begin{pmatrix} 0 & 0 & 1 \\ 0 & 1 & 0 \\ 1 & 0 & 0 \end{pmatrix}$$

is the Hermitian form matrix. Then the orientation-preserving isometries of $\overline{\mathbb{H}^2_{\mathbb{C}}}$ are given in affine coordinates by

$$\mathrm{Isom}(\overline{\mathbb{H}^2_{\mathbb{C}}}) = \mathrm{PU}(3,\mathbb{C}),$$

the unitary group quotiented by $\pm I$.

For the rest of this section, we will work exclusively in the boundary $\partial\mathbb{H}^2_{\mathbb{C}}$. There are a few isometries that we are particularly interested in. A (*right*) *Heisenberg translation* by a point $(\xi, t) \in \mathscr{H}$ is given by

$$T_{(\xi,t)} = \begin{pmatrix} 1 & -\sqrt{2}\,\overline{\xi} & -|\xi|^2 + it \\ 0 & 1 & \sqrt{2}\xi \\ 0 & 0 & 1 \end{pmatrix}$$

These are isometries for all (ξ, t). A *complex dilation* by $\lambda \in \mathbb{C}$ is given by

$$D_\lambda = \begin{pmatrix} |\lambda|^2 & 0 & 0 \\ 0 & \lambda & 0 \\ 0 & 0 & 1 \end{pmatrix},$$

which is an isometry if and only if $|\lambda| = 1$. Note that, since the parameter λ is complex, this class of isometry corresponds to rotations about the z_1 axis. In modified horospherical coordinates, they are rotations about the v axis. Lastly, the *Korányi inversion* is an isometry defined by

$$\iota = \begin{pmatrix} 0 & 0 & 1 \\ 0 & -1 & 0 \\ 1 & 0 & 0 \end{pmatrix}.$$

These transformations are applied to a point in affine coordinates by left matrix multiplication, and normalization in the third coordinate in the case of the Korányi inversion.

We will also use the complex dilation above to transform from the unit Cygan sphere to other spheres, of possibly non-unit radius. For this purpose, we will take $\lambda \in \mathbb{R}^+$, since the argument of the parameter λ has no effect on the geometry of the sphere. Under this restriction, no non-trivial dilation D_λ is an isometry.

Each of the above transformations can also be written in modified horospherical coordinates:

$$T_{(\xi,t)}(\zeta, v) = \left(\zeta + \xi, v + t + 2\,\mathrm{Im}(\bar{\zeta}\xi)\right),$$
$$D_\lambda(\zeta, v) = (\lambda\zeta, |\lambda|^2 v),$$
$$\iota(\zeta, v) = \left(\frac{\zeta}{|\zeta|^2 - iv}, -\frac{v}{|\zeta|^4 + v^2}\right).$$

From our definition of the Heisenberg group in (8), Heisenberg translations are applied through *right* multiplication by elements of the group. It should be noted that it is also common for translations to be defined through left multiplication.

Each Cygan sphere has a one-dimensional object associated to it, known as a chain. For a Cygan sphere of center (ξ, t) and radius $\lambda > 0$, its associated *chain* is defined as

$$C = T_{(\xi,t)} D_\lambda C_0,$$

where $C_0 = S_1 \times 0$ is the *standard chain*. We call C the chain of center (ξ, t) and radius λ.

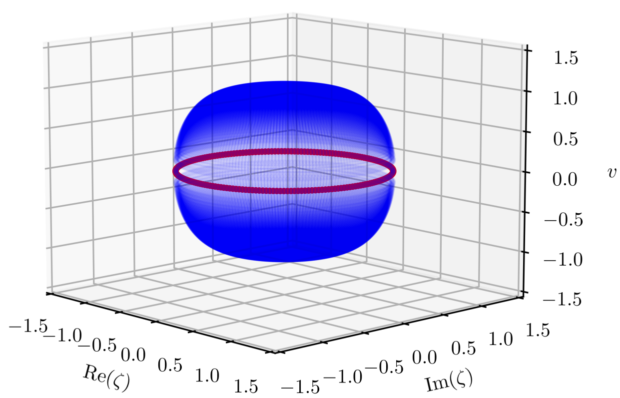

Figure 7: The unit Cygan sphere, centered at the origin (blue), and the standard chain (red), in $\partial\mathbb{H}^2_{\mathbb{C}}$. Compared to the Euclidean sphere, this sphere has a flatter top and bottom.

For a given Cygan sphere in $\partial\mathbb{H}^2_{\mathbb{C}}$, its associated chain contains all the same data, in the sense that the information about its center and radius are preserved. However, chains are generally easier to work with, and in particular, much easier to parameterize. Thus, we will speak of reflections through Cygan spheres in $\partial\mathbb{H}^2_{\mathbb{C}}$ and reflections through chains interchangeably.

In the real case, we expressed reflections through circles as isometries on $\mathbb{H}^2_{\mathbb{R}}$. The complex analogues of these circles are Cygan spheres, and their associated chains, in $\partial\mathbb{H}^2_{\mathbb{C}}$. For a chain C of center (ξ, t) and radius λ, the *complex reflection* through it is defined by the composition of transformations,

$$\iota_C = T_{(\xi,t)} D_\lambda \iota D_{\lambda^{-1}} T_{(-\xi,-t)}. \tag{9}$$

Taking $\lambda = 1$ and $(\xi, t) = (0,0)$, we find that the Korányi inversion is the complex reflection through the standard chain, C_0.

4.2 Complex Kleinian Groups

Here, we consider a generalization of the classical Kleinian groups described in §3.2. A *higher dimensional complex Kleinian group*, or simply a *complex Kleinian group*, is a discrete subgroup of $\mathrm{PSL}(n+1,\mathbb{C})$ which acts on $\mathbb{P}^n_{\mathbb{C}}$ with a nonempty region of discontinuity.

Before discussing specific examples, we develop a few important concepts. In the real hyperbolic case, we used the derivatives of the reflections to compute the entries of the transition matrix T. In the complex case, we instead use the square rooted determinant of the Jacobian matrix. The following is an essential result for implementing this computationally:

Lemma 4.1 ([6]). *If ι_C is the complex reflection through the chain of center (ξ, t) and radius λ, let J_C denote the Jacobian matrix of ι_C with respect to the real variables x, y, v with $x + iy = \zeta$. Let $J_C(\zeta_0, v_0)$ denote the Jacobian evaluated at a particular point in $\mathscr{H}$, and let $|\cdot|$ denote the absolute value of the determinant. Then*

$$\sqrt{\left|J_C(\zeta_0, v_0)\right|} = \frac{\lambda^4}{d_{cyg}((\zeta_0, v_0)(\xi, t))^4}.$$

Proof. We will compute the Jacobian determinant for the component functions of ι_C in (9), then apply the chain rule. For the Korányi inversion, we have in real variables that

$$\iota(x,y,z) = \left(\frac{x(x^2+y^2) - yv}{(x^2+y^2)^2+v^2}, \frac{y(x^2+y^2)+xv}{(x^2+y^2)+v^2}, -\frac{v}{(x^2+y^2)^2+v^2}\right).$$

Then, the Jacobian determinant of ι at $(x_0 + iy_0, v_0) \in \mathscr{H}$ is

$$\begin{aligned}\sqrt{\left|J_{C_0}(\zeta_0, v_0)\right|} &= \frac{1}{(x_0^2+y_0^2)^2+v_0^2} \\ &= \frac{1}{d_{cyg}((x_0+iy_0, v_0), (0,0))^4}.\end{aligned}$$

So, the claim holds for $C = C_0$. Now, we compute that

$$\begin{aligned}\sqrt{\left|T_{(\xi,t)}(\zeta_0, v_0)\right|} &= 1, \\ \sqrt{\left|D_\lambda(\zeta_0, v_0)\right|} &= \lambda^2.\end{aligned}$$

Both of these are constant on $\mathscr{H}$. So, by the chain rule,

$$\begin{aligned}
\sqrt{\left|J_C(\zeta_0, v_0)\right|} &= \sqrt{\left|J_{T_{(\xi,t)}} \cdot J_{D_\lambda} \cdot J_\iota\big(D_{\lambda^{-1}} \circ T_{(-\xi,-t)}(\zeta_0, v_0)\big) \cdot J_{D_{\lambda^{-1}}} \cdot J_{T_{(-\xi,-t)}}\right|} \\
&= \sqrt{\left|J_\iota\left(\lambda^{-1}(\zeta_0 - \xi), \lambda^{-2}\left[v_0 - t + 2\,\mathrm{Im}(\overline{\zeta_0}\xi)\right]\right)\right|} \\
&= \frac{1}{d_{cyg}(\left(\lambda^{-1}(\zeta_0 - \xi), \lambda^{-2}\left[v_0 - t + 2\,\mathrm{Im}(\overline{\zeta_0}\xi)\right]\right), (0,0))^4} \\
&= \frac{\lambda^4}{d_{cyg}((\zeta_0, v_0)(\xi, t))^4}.
\end{aligned}$$

□

It will also be useful to know, given a complex reflection and a chain, where that chain is mapped to under the reflection. This is important both in tracking the Cygan spheres in each refinement, and in checking the condition $i \mapsto j$ in the algorithm.

Define $\eta : \mathscr{H} \to \mathbb{C}$ by

$$\eta(\zeta, v) = |\zeta|^2 + i v.$$

Then

$$d_{cyg}\big((\zeta_1, v_1), (\zeta_2, v_2)\big)^2 = \left|\eta\big((\zeta_1, v_1) * (\zeta_2, v_2)^{-1}\big)\right|.$$

With some computation, we obtain the following:

Proposition 4.1. Let C denote the chain of center (ξ, t) and radius λ, and let C' denote the chain of center (μ, x) and radius ρ. Let α and (β, γ) denote the radius and center of the image of C under the reflection through C'. Define

$$\nu = \frac{1}{\rho^2 - \eta\big((\xi, t) * (\mu, x)^{-1}\big)}.$$

Then

$$\begin{aligned}
\alpha &= \lambda^2 \rho\, |\nu|, \\
\beta &= \xi + \lambda^2 \nu(\xi - \mu), \\
\gamma &= t - 2\lambda^2\,\mathrm{Im}\left[\,\overline{\xi}\,\nu(\xi - \mu)\right] + \lambda^4 \nu^2 \left(t - x - 2\,\mathrm{Im}(\overline{\xi}\mu)\right).
\end{aligned}$$

4.3 A Symmetric Example

In this example, we consider a symmetric Kleinian group of variable size, as determined by a real parameter $\theta \in (0, \pi/3)$. The generators of this group consist of reflections through three Cygan spheres with identical radii, centered in the ζ-plane. Denote the third roots of unity by

$$(w_0, w_1, w_2) = (1, e^{2\pi i/3}, e^{4\pi i/3}).$$

The spheres of this group have radii equal to $\tan(\theta)$, and centers at $(\sec(\theta), 0)$, $(w_1 \sec(\theta), 0)$, and $(w_2 \sec(\theta), 0)$ in $\mathscr{H}$. This group is symmetric under rotation by $2\pi/3$ about the v axis. For $s \in [0, 2\pi)$, the associated chains are parameterized by

$$\begin{aligned}
C_1 &= \left(\sec(\theta) + \tan(\theta)e^{is}, -2\sin(s)\tan(\theta)\sec(\theta)\right),\\
C_2 &= \left(w_1 \sec(\theta) + \tan(\theta)e^{is}, -2(\sqrt{3}\cos(s) - \sin(s))\tan(\theta)\sec(\theta)\right),\\
C_3 &= \left(w_2 \sec(\theta) + \tan(\theta)e^{is}, 2(\sqrt{3}\cos(s) + \sin(s))\tan(\theta)\sec(\theta)\right).
\end{aligned}$$

The group is plotted in figure 8. We next want to obtain an asymptotic estimate for the

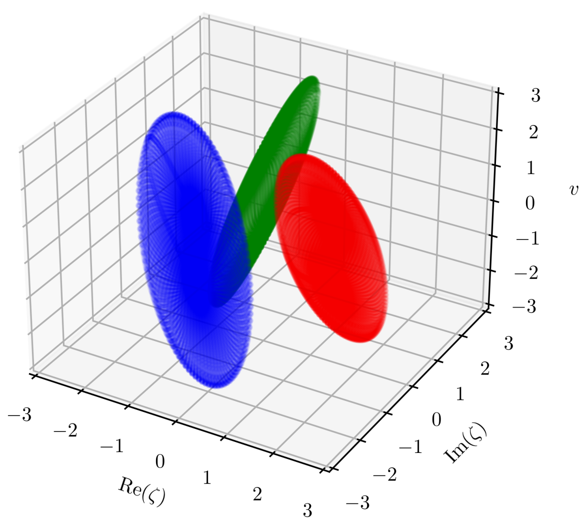

Figure 8: The Cygan spheres of the symmetric group with $\theta = \pi/4$, plotted in red, green, and blue.

dimension of the limiting set of this group. Let (ξ_i, t_i) denote the center of the i-th chain. Using lemma 4.1, for $i \neq j$ we obtain

$$\begin{aligned}
\sqrt{\det\left(J_{C_i}(\xi_j, t_j)\right)} &= \frac{\tan^4(\theta)}{d_{cyg}((\xi_i, t_i), (\xi_j, t_j)^4}\\
&= \frac{\tan^4(\theta)}{(\sqrt{3}\sec(\theta))^4 + (\sqrt{3}\sec^2(\theta))^2}\\
&= \frac{\sin^4(\theta)}{12}.
\end{aligned}$$

The transition matrix is thus given by

$$T = \frac{\sin^4(\theta)}{12}\begin{pmatrix} 0 & 1 & 1 \\ 1 & 0 & 1 \\ 1 & 1 & 0 \end{pmatrix}.$$

Then, we desire α such that the largest eigenvalue of T^{α} is $2\left(\frac{\sin^4(\theta)}{12}\right)^{\alpha} = 1$. Solving for α, we obtain

$$\alpha = \frac{\log(2)}{\log(12) - 4\log(\sin(\theta))}.$$

This estimate is more accurate for small θ. Now, we present numerical results. Using the eigenvalue algorithm, we computed the Hausdorff dimension of the limiting set of the symmetric Kleinian group, for various choices of θ. We took three refinements in the algorithm. In figure 9, we compare these results with the asymptotic estimate.

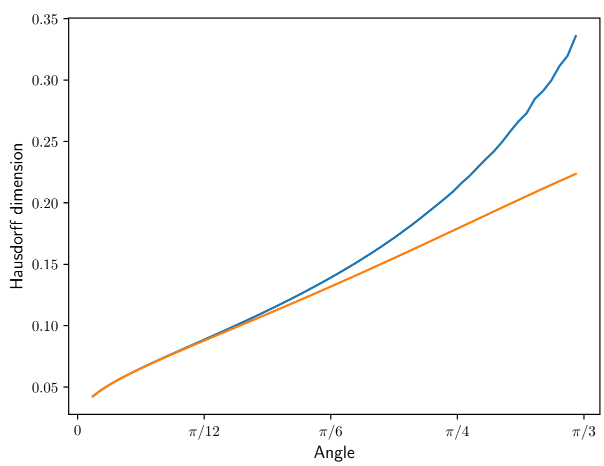

Figure 9: Numerically computed Hausdorff dimension (blue) and dimension estimated by the asymptotic formula (orange).

4.4 A Non-Symmetric Example

Next, we consider a non-symmetric Kleinian group of variable size, as determined by a real parameter $\theta \in (0, 9\pi/40)$. Here the maximum angle, $9\pi/40$, is chosen so that the Cygan spheres of the group do not intersect. Two of the spheres are centered at opposite points on the v axis, at $(0, \sec^2(\theta))$ and $(0, -\sec^2(\theta))$ The third sphere is centered in the ζ-plane at $(-i\sec(\theta), 0)$. All three spheres have radius $\tan(\theta)$. The chains in this group are parameterized by

$$C_1 = \left(\tan(\theta)e^{is}, \sec^2(\theta)\right),$$
$$C_2 = \left(\tan(\theta)e^{is}, -\sec^2(\theta)\right),$$
$$C_3 = \left(\tan(\theta)e^{is} - i\sec(\theta), -2\tan(\theta)\sec(\theta)\cos(s)\right),$$

for $s \in [0, 2\pi)$. The group is plotted in figure 10. Now, we obtain an asymptotic estimate

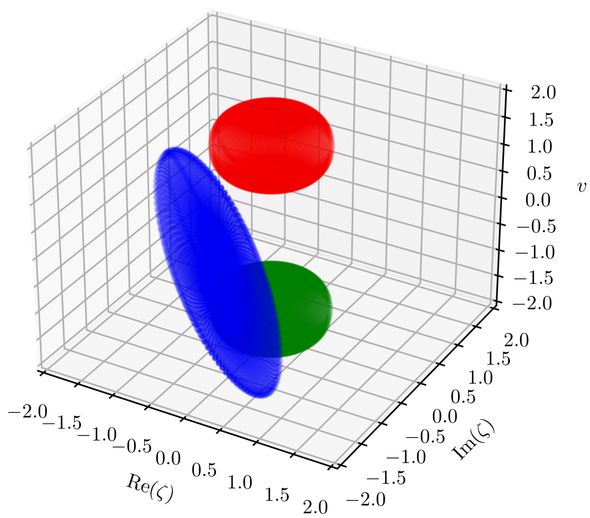

Figure 10: The Cygan spheres of the non-symmetric group with $\theta = \pi/5$, plotted in red, green, and blue.

for the dimension in this case. Since this group is non-symmetric, the structure of the transition matrix will not be as simple as in §4.3. Let (ξ_i, t_i) denote the center of C_i. For $i \neq j$, the entries of the transition matrix are given by

$$\begin{aligned} T_{ij} &= \sqrt{\det(J_{C_i}(\xi_j, t_j))} \\ &= \frac{\tan^4(\theta)}{d_{cyg}((\xi_i, t_i), (\xi_j, t_j))^4} \\ &= \begin{cases} \frac{1}{4}\sin^4(\theta) & (i, j) \in \{(1,3), (3,1)\}, \\ \frac{1}{2}\sin^4(\theta) & \text{otherwise.} \end{cases} \end{aligned}$$

Then

$$T = \frac{1}{2}\sin^4(\theta)\begin{pmatrix} 0 & 1 & 1/2 \\ 1 & 0 & 1 \\ 1/2 & 1 & 0 \end{pmatrix}.$$

A bit of computation shows that the largest eigenvalue of T^{α} is then given by

$$\frac{\sin^4(\theta)}{2}\left(2^{-2\alpha}+\sqrt{2^{3-2\alpha}+2^{-4\alpha}}\right)=1.$$

As in §3.4, this problem is difficult to solve analytically, but we can obtain a numerical solution via root finding. We computed the Hausdorff dimension of the limit set for this group, with 3 refinements. Figure 11 provides a comparison between the computed dimension and the asymptotic dimension.

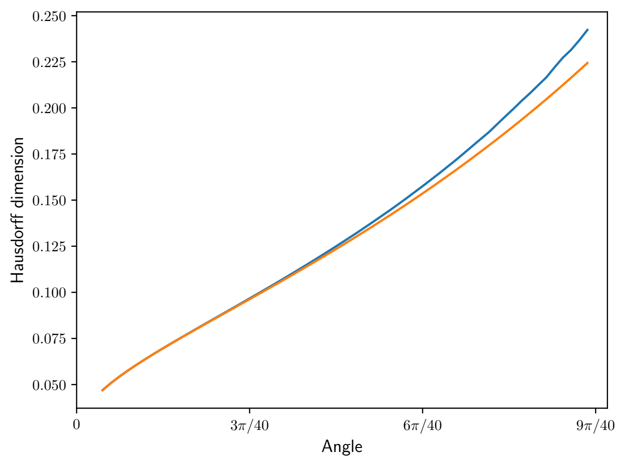

Figure 11: Numerically computed dimension (blue) and dimension estimated by asymptotic formula.

Acknowledgements

We would like to thank Dr. Hadrian Quan and PhD student Raghavendra Tripathi for their teaching, guidance, and mentorship through this project. We also wish to thank the Washington Experimental Mathematics Lab and Professor Christopher Hoffman for supporting our research.

References

[1] A. Cano, J. Navaratte, J. Seade. *Complex Kleinian Groups*, volume 303 of *Progress in Mathematics*. Birkhäuser, 2013.

[2] A. Cano and J. Seade. *An Overview of Complex Kleinian Groups*, volume 11 of *Nonlinear Systems and Complexity*, page 167–194. Springer, Cham, 2015. In: Nonlinear Dynamics and New Directions by González-Aguilar, H. and Ugalde, E.

[3] W. Goldman and J. Parker. Dirichlet Polyhedra for Dihedral Groups Acting on Complex Hyperbolic Space. *The Journal of Geometric Analysis*, 2(6), 1992.

[4] P.L. Krapinsky and E. Ben-Naim. Multiscaling in Stochastic Fractals. *Physics Letters A*, 196, 1994.

[5] C. McMullen. Hausdorff Dimension and Conformal Dynamics III: Computation of Dimension. *American Journal of Mathematics*, 120(4), 1997.

[6] S. Romaña and A. Ucan-Puc. On McMullen's Algorithm for the Hausdorff Dimension of Complex Schottky Groups. *Geometriae Dedicata*, 2021.

[7] J. Seade and A. Verjovsky. Higher Dimensional Kleinian Groups. *Mathematische Annalen*, 322, 2002.

[8] G. Sienra. Complex Kleinian Groups and Limit Sets in P^2. *Complex Variables, Theory, and Applications: An International Journal*, 49(10), 689-701.

Jacob Linden
University of Chicago
`jacoblinden@uchicago.edu`

Xuqing Wu
University of Pennsylvania
`xuqingwu@upenn.edu`